Supporting Information

Mn^{2+} Doping Enables Improved Crystallization of $CsPbI_3$ Quantum Dots for Efficient Deep-red Light-emitting Diodes

Mengyun Liu [a,b], *Jing Zhou* [a,b], *XueRong Hao* [a,b], *Hongli Liu* [a,b,*], *Shirong Wang* [a,b], *Xianggao Li* [a,b,*]

a School of Chemical Engineering and Technology, Tianjin University, Tianjin 300072, China

b Collaborative Innovation Center of Chemical Science and Engineering (Tianjin), Tianjin 300072, China

Corresponding Author

*Email: liuhongli@tju.edu.cn(H. L.)

*Email: lixianggao@tju.edu.cn(X.L.)

Materials and methods

Materials

Cesium carbonate (Cs_2CO_3, aladdin, ≥99%), Lead diacetate trihydrate (Pb $(CH_3CO_2)_2$. $3H_2O$, meryer, ≥99.999%), manganese acetate (Mn $(OAc)_2$, aladdin,98%), oleic acid (OA, energy chemical,90%), oleylamine (OLA, aladdin,80%-90%),1-octadecene (1-ODE, energy chemical, 90%), benzoyl chloride (Bz-Cl, aladdin, 99%), sodium iodide (NaI, meryer, 99.99%), hexane (Aladdin, >99%), methyl acetate (Aladdin, >99%). PTAA、PEDOT: PSS (Al 4083), and TPBi (99.999%) were purchased from Xi'an Polymer Light Technology Corp. All chemicals were used as received without further purification

Preparation of Benzoyl iodide (Bz-I).

The reaction was performed in a N_2-filled glovebox following the procedure reported [1]. In short, sodium iodide (3 g) was mixed with benzoyl chloride (1.5 mL) in a 20 mL vial. The mixture was vigorously stirred at 75 ℃ on a hot plate for 5 h. The reaction mixture turned from colorless to an orange-red color, indicating that the transformation of the benzoyl chloride into the benzoyl iodide was successful. Next, the reaction mixture was cooled down to RT. Finally, the solution was filtered, using a polytetrafluorethylene membrane filter with a 0.45 um pore size, in order to collect the liquid precursor.

The synthesis of $CsPbI_3$ quantum dots (QDs).

$CsPbI_3$ QDs were synthesized by modifying a colloidal hot-injection approach developed for other lead metal halide QDs. 0.1 mmol cesium carbonate and 0.4 mmol Lead diacetate trihydrate, 2 ml OA, 2 ml OLA and 10 ml 1-ODE were put into a three-neck flask and dried for 110 ℃ for 1h under vacuum condition. The temperature was then increased to 165 ℃ under nitrogen atmosphere. Afterward, 200 uL of Bz-I dispersed in 0.4 mL of degassed 1-ODE was swiftly injected inside the flask. The reaction was quenched after 10 s by using an ice bath. Finally, 10 mL of hexane was

added to the crude NCs solution, which was centrifuged at 10000 rpm for 5 min. The final QDs were obtained in the following way: the precipitate was redispersed in 3 mL of hexane and the NCs in the supernatant were precipitated by the addition of 6 mL of ethyl acetate and centrifugation at 10000 rpm for 5 min. Then, the precipitate was redispersed in 2 mL of hexane and the QDs in the supernatant were precipitated by the addition of 4 mL of ethyl acetate and centrifugation at 10000 rpm for 5 min. Finally, the precipitate was dispersed in octane (0.5 ml) and stored in centrifugal tube for further use.

The synthesis of Mn^{2+}-doped $CsPbI_3$ QDs

The synthesis of Mn^{2+}-doped $CsPbI_3$ QDs is similar to $CsPbI_3$. Manganese acetate (0.08, 0.10, 0.13, and 0.20 mmol) and Lead diacetate trihydrate (0.32, 0.30, 0.27, and 0.20 mmol), were added into the solution including (0.1 mmol Cs_2CO_3, 10 ml 1-ODE, 2 ml OA, 2ml OLA), respectively. The post-processing procedures were carried out as described above.

Device fabrication.

Patterned ITO-coated glass substrates were cleaned with deionized water, ethyl alcohol, acetone, isopropanol, and ethyl alcohol in sequence by sonication and then dried with nitrogen and treated with oxygen plasma for 10 min at 80 W. All the devices were fabricated with a typical multilayer structure consisting of ITO/PEDOT: PSS/PTAA/Perovskite/TPBi/LiF/Al. The PEDOT: PSS solution was filtered with 0.22 μm hydrophilic filters before use. Then PEDOT: PSS was spin-coated onto ITO at 4000 rpm for 30 s and annealed for 15 min at 140 ℃ in the atmospheric environment. PTAA (dissolved in chlorobenzene, 4 mg mL^{-1}) solution was spin-coated onto PEDOT: PSS films at 4000 rpm for 30 s and annealed for 15 min at 140 ℃. Then, the substrates were transferred into an Ar-filled glovebox, and PeQDs colloidal solution was spin-coated on the PTAA layer at 2000 rpm for 30 s and annealed for 5 min at 80 ℃. On the top of the PeQDs layer, TPBi (40 nm, 1–2 Å/s), LiF (1 nm, 0.1–0.2 Å/s), and Al (100 nm, 8–10 Å/s) were sequentially deposited by thermal evaporation. The effective luminous area of the PeQLEDs is 2 × 3 mm^2 which was defined by the overlapping of ITO and

Al electrode.

Characterization

Ultraviolet–visible (UV–vis) absorption spectra were measured by Thermo Evolution 300 UV–vis spectrometer. Steady-state photoluminescence (PL) spectra, time resolution photoluminescence (TRPL) spectra, and absolute photoluminescence quantum yield (PLQY) were carried out by a Horiba Fluorolog system with an excitation wavelength of 365 nm and a 375 nm nano-LED source. Film thickness data was obtained using KLA Instruments probe profilometer Tencor D-300. Impedance data was collected by the Shanghai Chenhua electrochemical workstation (chi660e). X-ray diffraction (XRD) patterns were characterized by Rigaku Miniflex 600 with Cu Kα radiation (λ = 1.54178 Å). Transmission electron microscope (TEM) was performed by JEM-2100F at 200 kV accelerating voltage. The energy level was obtained by a Thermo ESCALAB 250Xi ultraviolet photoelectron spectroscopy (UPS) (The Valance band spectra were measured with a monochromatic He I light source (21.2 eV) and a VG Scienta R4000 analyzer. X-ray photoelectron spectroscopy (XPS) spectra were recorded by a Thermo ESCALAB-250 spectrometer. The luminescence-current density-voltage (L-J-V) characteristics were recorded by a commercial system (Keithley 2400 source meter and photodetector, Guangzhou Jinghe Equipment Co., Ltd) under an Ar atmosphere. The response time of the photodetector is about 50 ns and the scan length was set as 0.2 V. The Electroluminescence (EL) spectra and CIE coordinate measurements were conducted and recorded by Chroma meter CS-2000.

Calculations of average PL lifetimes.

All TRPL decay curves were nearly biexponential and measured at the corresponding PL emission spectra with the excitation wavelength of 395 nm. The corresponding fitting formula was supplied as follows[2]:

$$I_t = I_1 e^{(-t/\tau_1)} + I_2 e^{(-t/\tau_2)}$$

The average PL lifetimes can be calculated by function as:

$$\tau_{avg} = (I_1\tau_1^2 + I_2\tau_2^2)/(I_1\tau_1 + I_2\tau_2)$$

To explore the kinetic decay process, the radiative rate of perovskite QDs and its non-radiative decay rate are calculated by adopting the photoluminescence quantum yields (PLQYs) and τ_{avg} of the samples. The radiative recombination rate (k_r) and the nonradiative recombination rate (k_{nr}) can be calculated:

$$K_r = \frac{PLQY}{\tau_{avg}}$$

$$K_{nr} = \frac{1 - PLQY}{\tau_{avg}}$$

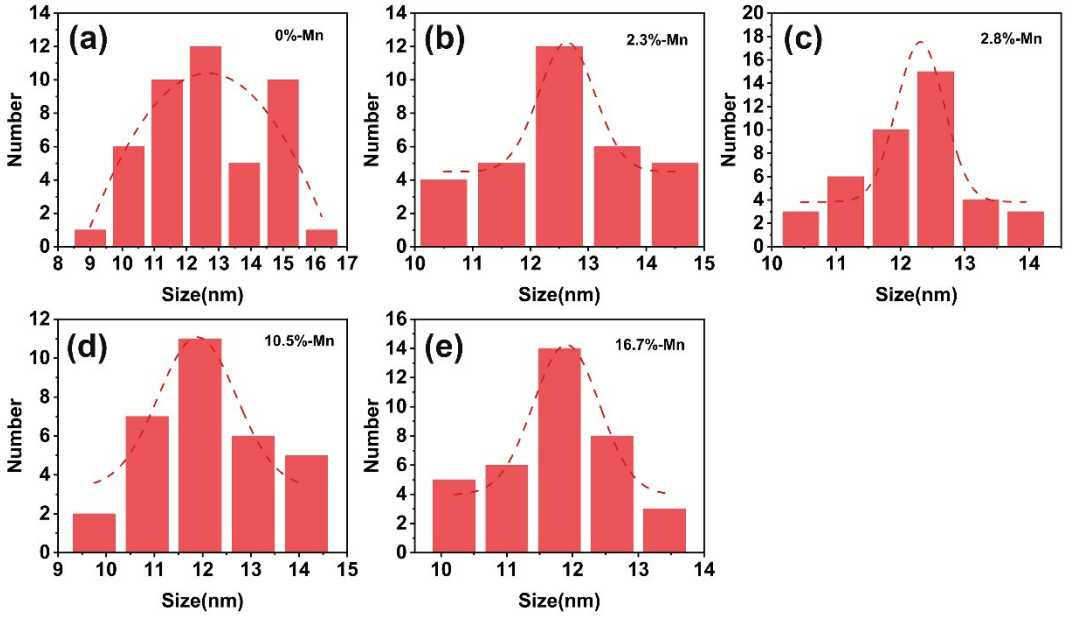

Figure S1 (a)-(e) Particle size distribution of $CsPb_{1-x}Mn_xI_3$ (x=0, 0.023, 0.028, 0.105 and 0.167) QDs.

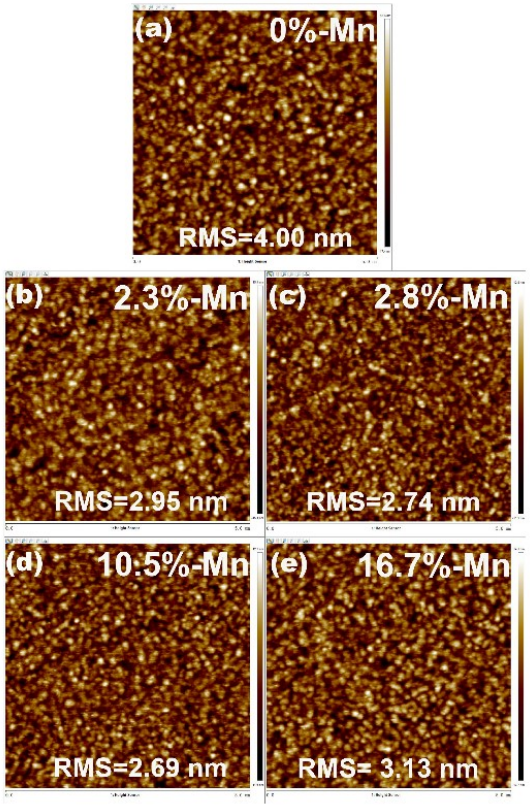

Figure S2 AFM images of $CsPb_{1-x}Mn_xI_3$ (x=0, 0.023, 0.028, 0.105, and 0.167) QDs.

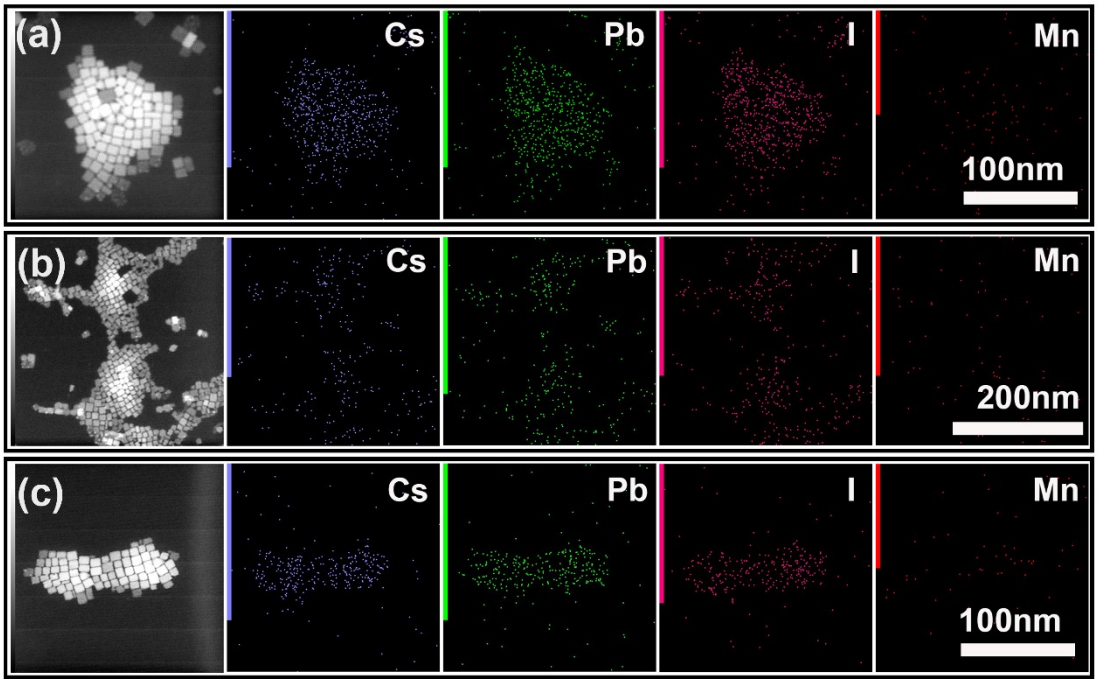

Figure S3 (a) EDS plots of the $CsPb_{0.972}Mn_{0.028}I_3$ QDs. (b) EDS plots of the $CsPb_{0.895}Mn_{0.105}I_3$ QDs. (c) EDS plots of the $CsPb_{0.833}Mn_{0.167}I_3$ QDs.

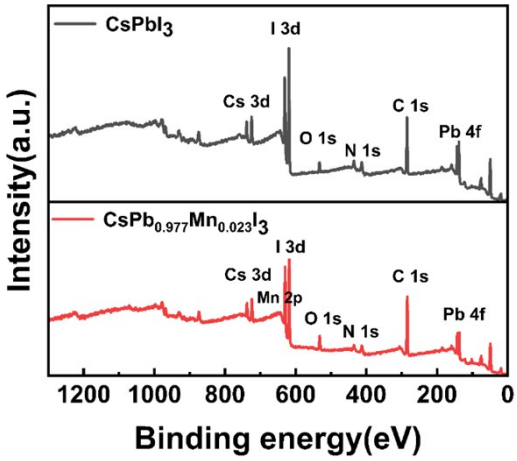

Figure S4 XPS full spectra of $CsPbI_3$ and $CsPb_{0.977}Mn_{0.023}I_3$ QDs.

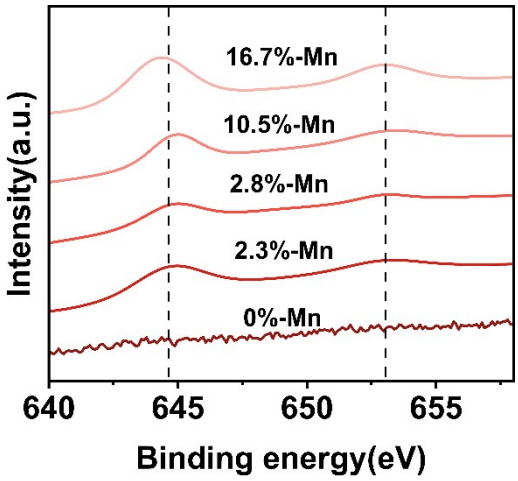

Figure S5 XPS spectra of $CsPb_{1-x}Mn_xI_3$ (x = 0, 0.023, 0.028, 0.105, and 0.167) QDs of Mn 2p.

Table S1 XPS elemental binding energies of CsPb1-xMnxI$_3$ (x = 0, 0.023, 0.028, 0.105 and 0.167)

Sample	Pb $4f_{5/2}$ (eV)	Pb $4f_{7/2}$ (eV)	Cs $3d_{3/2}$ (eV)	Cs $3d_{5/2}$ (eV)	I $3d_{3/2}$ (eV)	I $3d_{5/2}$ (eV)
$CsPbI_3$	142.18	137.38	737.58	723.59	629.68	618.15
$CsPb_{0.977}Mn_{0.023}I_3$	142.43	137.58	737.78	723.85	629.78	618.35
$CsPb_{0.972}Mn_{0.028}I_3$	142.28	137.48	737.78	723.82	629.75	618.28
$CsPb_{0.895}Mn_{0.105}I_3$	142.28	137.43	737.79	723.82	629.71	618.25
$CsPb_{0.833}Mn_{0.167}I_3$	142.28	137.38	737.78	723.80	629.68	618.21

Table S2 Short lifetimes (τ_1), long lifetimes (τ_2) and average lifetimes (τ_{avg}) of $CsPb_{1-x}Mn_xI_3$ (x = 0, 0.023, 0.028, 0.105 and 0.167)

Sample	τ_1(ns)	τ_2(ns)	f1(%)	f2(%)	τ_{avg}(ns)
$CsPbI_3$	23.9	52.6	63	37	34.4
$CsPb_{0.977}Mn_{0.023}I_3$	32.4	75.9	74	26	43.8
$CsPb_{0.972}Mn_{0.028}I_3$	28.0	73.3	75	25	39.5
$CsPb_{0.895}Mn_{0.105}I_3$	24.7	56.0	67	33	35.2
$CsPb_{0.833}Mn_{0.167}I_3$	23.5	53.9	77	23	30.5

Table S3 Average lifetimes (τ_{avg}), PLQY, k_r, k_{nr}, and k_r/k_{nr} of $CsPb_{1-x}Mn_xI_3$ (x = 0, 0.023, 0.028, 0.105 and 0.167)

Sample	τ_{avg} (ns)	PLQY (%)	k_r (10^7 s^{-1})	k_{nr} (10^7 s^{-1})	k_r/k_{nr}
$CsPbI_3$	34.4	43.83	1.27	1.66	0.76
$CsPb_{0.977}Mn_{0.023}I_3$	43.8	58.00	1.32	0.96	1.28
$CsPb_{0.972}Mn_{0.028}I_3$	39.5	49.80	1.26	1.27	0.96
$CsPb_{0.895}Mn_{0.105}I_3$	35.2	41.79	1.18	1.65	0.71
$CsPb_{0.833}Mn_{0.167}I_3$	30.5	41.59	1.36	1.91	0.71

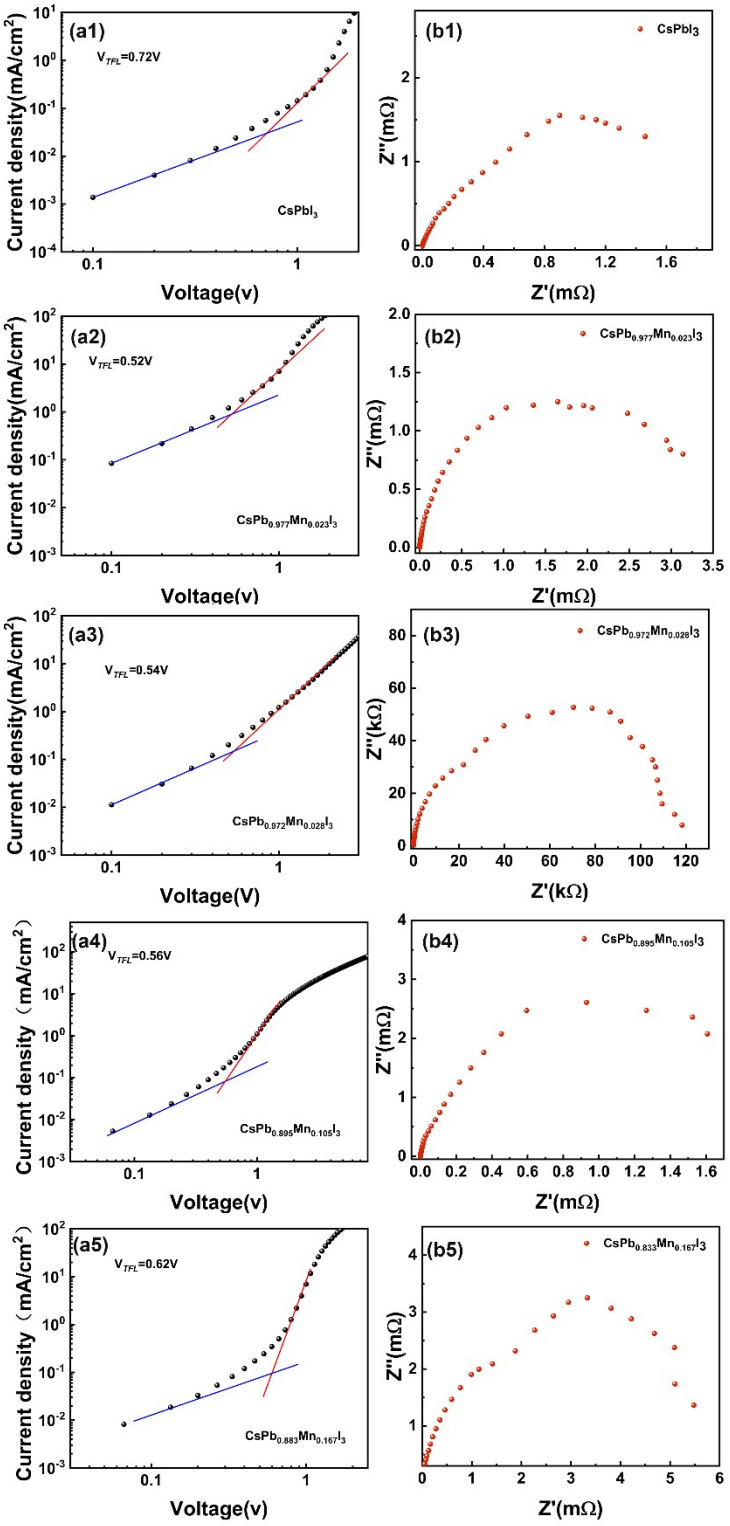

Figure S6 (a1)-(a5) *J-V* curves of hole single-loaded devices with $CsPb_{1-x}Mn_xI_3$ (x = 0, 0.023, 0.028, 0.105 and 0.167) QDs as the luminescent layer under dark current; (b1)-(b5) Nyquist plots of ITO/PEDOT: PSS/PTAA/QDs/TPBi/Al device structures simulated to compute the relative permittivity of $CsPb_{1-x}Mn_xI_3$ (x = 0, 0.023, 0.028, 0.105 and 0.167) QDs.

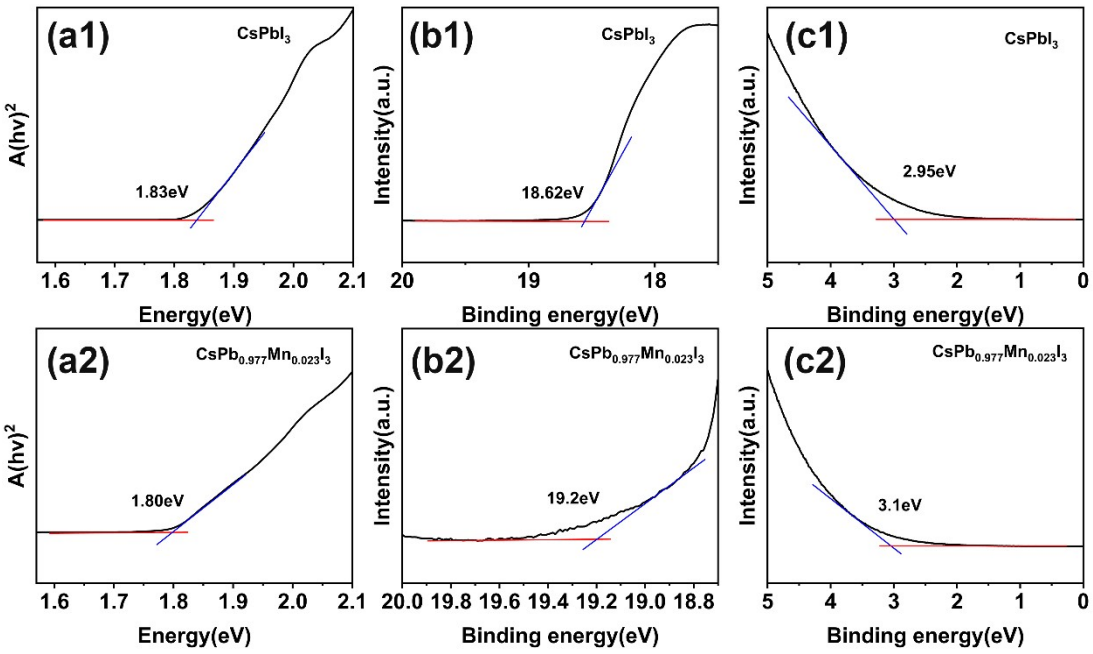

Figure S7 (a) Tauc plots of $CsPbI_3$ (a1) and $CsPb_{0.977}Mn_{0.023}I_3$ (a2). b, c) Ultraviolet photoelectron spectroscopy (UPS) spectra of $CsPbI_3$ (b1, c1) and $CsPb_{0.977}Mn_{0.023}I_3$ (b2, c2). The UPS results were calibrated using etched and surface-cleaned Au as a calibration.

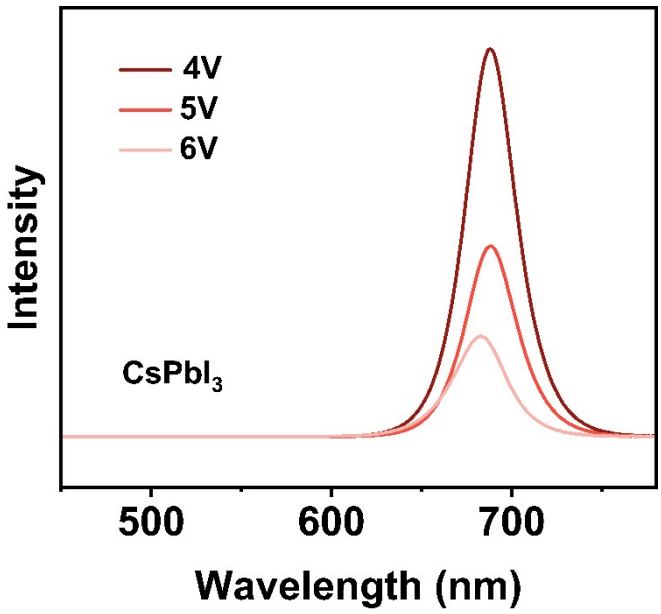

Figure S8 Electroluminescence spectrum of $CsPbI_3$ QDs-based PeLEDs at different voltages under continuous operation.

1. M. Imran, V. Caligiuri, M. Wang, L. Goldoni, M. Prato, R. Krahne, L. De Trizio and L. Manna, *Journal of the American Chemical Society*, 2018, **140**, 2656-2664.

2. S. Zhang, H. Liu, X. Li and S. Wang, *Nano Energy*, 2020, **77**.